A Real Test and Simulation Result Comparison of Selected Properties of Hybrid Composite Materials

Naqib Daneshjo

Faculty of Commerce, University of Economics in Bratislava, Slovak Republic
daneshjo47@gmail.com

Dusan Sabadka

Faculty of Mechanical Engineering, Technical University of Kosice, Slovak Republic
dusan.sabadka@tuke.sk

Peter Malega

Faculty of Mechanical Engineering, Technical University of Kosice, Slovak Republic
peter.malega@tuke.sk (corresponding author)

ABSTRACT

In this study, the notion of composite materials is thoroughly assessed. Actual and simulation in a specific computer software stress testing of hybrid composites are investigated. The paper deals with the mechanics of rigid bodies, their elasticity, strength, and stiffness. In addition to a general overview of the former's behavior and properties, this paper presents the possibility of calculating the bearing capacity of various materials in relevant computer programs. The production and testing process of the composite samples are described. The latter are then subjected to simulated tests in computer software. The main objective of this study is to compare real test results of hybrid composites, namely combined carbon fibers, glass fibers, aramid-carbon fibers, aramid honeycomb, and metal mesh with the simulation findings.

Keywords-simulation; composite materials; hybrid composites; tensile test; simulation of tensile test

I. INTRODUCTION

The development of new technologies has imported various materials into the production market, which have not been frequently used so far mostly due to their high cost or demanding production process. A typical example of such materials is modern hybrid composites [1-4], which mainly attain excellent parameters of mechanical resistance while maintaining low weight. The need for decreased prices and the necessity to implement new materials into practice owing to their unique properties indicate that the latter will be more frequently used in the future [5-8]. Thus, newly designed components and other structural elements made from them need to be tested. Since the main limiting factor is still the high cost, testing many samples is financially demanding, whereas special equipment and qualified personnel are required to carry out these tests. This constitutes a major obstacle in the case of a limited budget [9-12]. A possible solution might be to replace the practical tests of mechanical properties with a simulated test in a computer interface while using a specific calculation method [13-15].

Hybrid composite materials, combining different types of fibers and matrices, have become increasingly popular in various engineering applications due to their unique property combination. The comparison of properties obtained from real tests with those acquired through simulation programs is critical for ensuring the accuracy and reliability of computational models, therefore facilitating material design and optimization [16-19]. In [20-22], tensile and bending tests on hybrid composite specimens were conducted and the results were compared with those obtained from finite element analysis (FEA). A good agreement between experimental and simulated stress-strain curves was found, validating the predictive capabilities of the FEA model. Authors in [23-25] investigated the impact behaviour of hybrid composite laminates using both experimental testing and cohesive zone modeling. By comparing the delamination patterns observed in experiments with those predicted by simulation, they gained insights into the mechanisms governing interlaminar fracture in hybrid composites. In [26-28], a multi-scale modeling approach was employed to optimize the microstructure of hybrid composite materials for enhanced mechanical properties. Through the comparison of simulation predictions

with experimental data, an optimal fiber orientation distribution that maximized the material's strength and stiffness was identified.

In this study, different types of hybrid composites were chosen as reference materials, which had already been subjected to tensile tests in a laboratory as part of another project. The goal is to compare the real test results with the ones obtained in simulations, so that a conclusion could be drawn from this comparison.

II.   USED MATERIALS FOR THE EXPERIMENT

Resin labelled L 285 MGS manufactured by Havel Composites was used as the matrix. This is a high-quality resin also employed in the aviation industry. A hardener from Havel Composites labelled 287 MGS was added to the resin in line with its intended purpose. A mixing ratio of 100:40 was utilized (with resin being the larger volume). The indicated time of possible processing after mixing these components is approximately 4 hours. The same matrix was applied for all reinforcements. All samples consist of seven layers symmetrically placed, with the outer 3 layers being the same each time: $2 \times$ carbon fabric and $1 \times$ glass fabric inward direction. The tested samples differ only in the middle layer through which the axis of symmetry passes. Carbon fabric represents the first, second, sixth and seventh layer of each tested sample. A product from the company Havel Composites was chosen with a stated weight of 160 g/m^2.
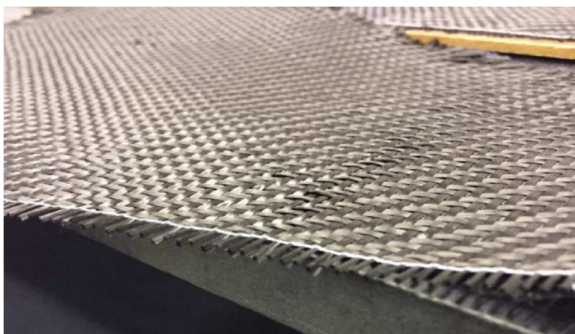

Fig. 1.   Carbon fabric used for sample production.

Glass fabric titled Aeroglass 110 (type E) with a density of 102 g/m^2 was used as the third, or the fifth layer for each of the samples produced for testing. At the same time, it was utilized as a middle specific layer for type A samples, where it was placed at an angle of 45° to achieve unique mechanical properties. It is about a third lighter than the carbon layer used, but at the same time it offers significantly lower values of the modulus of elasticity in tension, and its rupture occurs at roughly half the stress. Hybrid aramid-carbon fabric was applied as a middle layer for type C samples. It combines the properties of both types of fibres. Its density is stated as 165 g/m^2. As in the previous cases, the manufacturer is the company Havel Composites. Aramid honeycomb was chosen as a specific layer for type B samples. It is very light, has a density of only 48 g/m^2, which is mainly due to the large ratio of "empty" space to the aramid walls of the structure. It offers

interesting values of modulus of elasticity in tension and shear due to its low weight.

Fig. 2.   Glass fabric used in the production of the test samples.
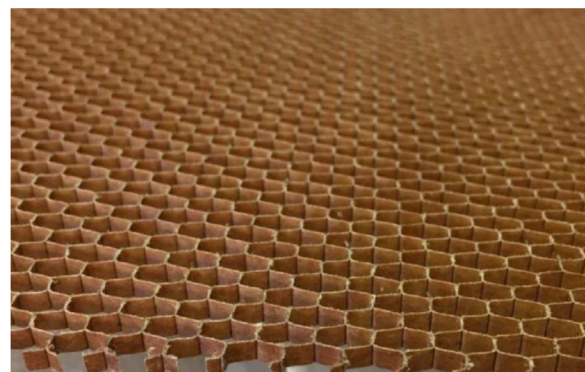

Fig. 3.   Detail of the aramid honeycomb that was used as the middle layer in the type B samples.

A metal grid with a mesh size of 2×2 mm was implemented as a specific layer in the type D sample. From the available information, we cannot determine the exact mechanical properties of this grid. A metal grid with a mesh size of 10×10 mm was chosen as a specific layer for the type D sample. Similar to the steel grid with a smaller mesh, in this case as well we cannot determine the exact mechanical properties of the material from the available information. For these samples, parameters for grids of the same size that could have been made of different steel will be used for simulation purposes.

Fig. 4.   Metal grid with a mesh size of 2×2 mm applied as a specific layer of D samples.
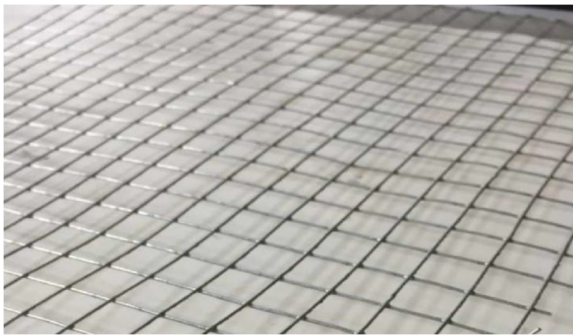
Fig. 5.   1 × 1 cm steel grid used for type E samples.

The materials needed for production were cut to a size of 26 × 33 cm. The matrix of resin and hardener were mixed according to the prescribed proportions. The individual layers, which were gradually stacked on top of each other, were subsequently saturated with the matrix. For the correct production of samples, it is necessary to observe the specified ratio of the matrix components and precisely stack the layers on top of each other. One of the last steps of the production procedure is the vacuuming, during which a layered sample is saturated with the matrix. This technology allows the removal of unwanted air from the sample, presses the individual layers together, and hardens the matrix. In practice, other technologies are additionally employed, being usually combined with increased ambient temperature during matrix hardening. After the matrix has hardened, the samples are milled from the individual composite "panels" with the assistance of special tools and they are then used in tests.

Fig. 6.   Samples prepared for the tensile test.

The testing was carried out according to the TS EN ISO 527 standard. The tearing device TIRAtest 2300 was used to conduct the tensile test of the produced samples, which consists of jaws into which the tested element is firmly clamped. One of the jaws usually stays firmly in place while the other acts on the sample with a gradually increasing force in one axis. The relative and total elongation of the sample is evaluated. To measure the elongation of a sample, the strain gauge is utilized. The maximum stress (force) that the sample can withstand without breaking is observed. Furthermore, various characteristics of flexibility, strength, and stiffness can be calculated. Elastic and plastic deformation as well as other attributes can be evaluated.

Fig. 7.   Broken samples after the tensile test.

Of the fifteen samples tested, three tests failed, namely sample types A, B, and E, where the sample has come loose from the pneumatic jaws. From the tensile test results, it was found that the greatest force F_m to break the material must be exerted on the type C samples. The hybrid component of the reinforcement mostly increases the force required to break the material. Tables I-V illustrate the test outcomes on the samples, while the average value of the 3 samples tested for one type is also given. For sample types A, B, and E, only two values were calculated. Type B samples achieved the lowest values. The glass fiber samples with different orientation had the highest ultimate tensile strength. On the other hand, type E samples with 10×10 mm metal grid achieved the lowest values of ultimate tensile strength. Regarding the type E samples, each of them experienced material failure in the jaw attachment area during testing, probably due to the size of the holes in the metal grid where deformation of the composite material due to jaw pressure occurred at the sample attachment point.

III.   TESTING COMPOSITE SAMPLES IN SIMULATION SOFTWARE

A key aspect before the actual modeling of composite samples and before their testing in simulation software takes place, is the knowledge of input parameters. These data should be as detailed and accurate as possible. During a later result evaluation it is useful to be aware of parameters that are not directly necessary for a specific calculation. While some data, such as tensile modulus, Poisson's number, specific density, etc., are provided by the material manufacturers themselves or can be drawn from other sources, several important input parameters must be calculated. Above all, it is necessary to know the material composition and dimensions of the sample that is to be subjected to the simulated load test. This study will be based on the values given in the previous project mentioned above as the source of samples.

The employed values of the sample dimensions could be verified by measuring as the tested samples are at this study's disposal. The problem is, however, that all samples were

subjected to tensile, possibly bending, test, during which they were irreversibly damaged. This makes it impossible for this research to accurately measure several dimensions. So, the former should rely on the data gathered from previous measurements. Recalculation of the thickness of individual layers is essential. The obtained thickness values will be utilized for modeling in the Abaqus program.

The type of matrix used, the share of its components during production, and their specific density, which is stated by the producer, are already known. The volume of the matrix that was used for individual layers is calculated based on specific density and weight. The thickness of the layer is determined by subsequently dividing the volume of the matrix by the area on which it was applied. The change in the density of the matrix after hardening must be considered. However, after rounding, it will not have a significant effect on the result. It is also necessary to consider the absorbency of the matrix reinforcement and the factor that a significant part of the applied matrix will fill the free space in the fabric to which it is applied. This phenomenon is most noticeable in sparsely woven reinforcements, such as the ones used in this study. The filling of the free space of the reinforcement in the case of metal grids or honeycombs is even more clearly observed. To calculate the thickness of the matrix, the thickness of the reinforcement is added, which significantly affects the result, especially when using metal and other grids with a relatively large diameter of the grid wire. The entire proposed formula for estimating the thickness of the layers would possibly be:

$$ t_i = \frac{m_i \cdot k_\rho \cdot k_i}{p_i \cdot S_i} + t\ reinforcement, i\ [mm] \qquad (1) $$

where m is the weight of the applied matrix [g], ρ is the specific density of the matrix obtained by calculation from the known specific densities of the individual components [kg/m^3], S is the area on which the matrix was applied [m^3], and k_ρ and k_i are the coefficients for the change in density after curing and for the saturation of the fabric. This formula will be applied when calculating layers containing fabrics. The thickness of the layers of metal grids and honeycombs is calculated from the known total thickness of the given sample by subtracting the calculated thicknesses of the other layers from the measured thickness of the sample.

For the calculations, the necessary input data are drawn from the datasheets of sellers and producers of materials, as well as the literature. After rounding, the following values were acquired:

- Thickness of the layer of saturated carbon fabric: 0.15 mm.

- Thickness of the layer of saturated glass fabric: 0.13 mm.

- Thickness of the saturated hybrid fabric layer: 0.15 mm.

- Thickness of the layer of saturated aramid honeycomb: 0.65 mm.

- Thickness of the layer of steel grid D and the matrix: 0.45 mm.

- Thickness of the layer of the steel grid E and the matrix: 1.02 mm.

All samples were produced by symmetrical layering and consist of seven layers. From both outer sides, the sample starts with two layers of carbon fabric, followed by a layer of glass fabric. This configuration is the same for all samples produced. At the core of the sample there is a specific layer that is different for each sample. Thus, the thickness of the individual tested samples varies only depending on the specific layer used in the core. The correctness of the previous considerations and calculations will be confirmed through experimental verification of the actual thickness of the tested samples.

IV. BASIC INPUT PARAMETERS OF THE MECHANICAL PROPERTIES OF THE MATERIALS USED

For correct simulation and to obtain accurate results corresponding to reality, it is crucial to know the material characteristics of flexibility, strength, and stiffness. In this study, for the simulation of the tensile test, the value of the modulus of elasticity in tension (Young's modulus), denoted as *E* [MPa] was utilized. Since composite materials are anisotropic, their behaviour depends on the direction in which the load is applied, the values of *E* for all 3 directions (in x, y, z axis) need to be known. These values are usually referred to as *E1, E2, E3*. The manufacturer of materials (Havel Composites) used to produce the examined samples without giving these parameters or used to provide only the parameters for unsaturated carbon fibers tested separately. However, in the official documentation for the materials, it is stated that the fabrics employed are produced in a license-certified manner. The original patent is owned by the company *Toray*, which lists the required values of mechanical characteristics. Materials should be produced from the same raw materials and with the same technology. So it will be assumed that the products produced under licenses do not differ qualitatively from the original ones. In case the manufacturer Toray indicates the parameters with a range of values, a counting with a lower value will be performed to compensate for a possible deficit in the quality of licensed fabrics.

Another important parameter is the Poisson´s number *μ* [-] and the modulus of elasticity in shear *G* [MPa]. As with *E* there are differences for individual directions. So values *μ1*, *μ2*, *μ3*, *G1*, *G2*, and *G3* will be needed. These values will be also drawn from the manufacturer. For a complex simulation and evaluation of the tensile test, additional parameters will be needed, which describe the behavior of the materials in the area of plastic deformations, above the yield point, at stresses close to the maximum bearing capacity of the sample. However, the available sources do not offer enough reliable information on materials used specifically in this study's case. Therefore, the focus of attention will be on assessing the area of elastic deformations within the tensile test in the simulation software.

Values *Ei*, *μi*, *Gi* for the honeycomb material, were additionally drawn from previous independent experiments, since the manufacturer did not provide all the necessary parameters. Input data for steel grids of given dimensions similarly came from experimental tests carried out by independent institutions. In this case, the situation was easier, as steel exhibits isotropic behavior. However, this does not apply perfectly, and isotropy depends on the production

technology. For this study's purposes, however, it is sufficient to conceptually idealize the material used.

Parameters of the modulus of elasticity in tension, or pressure of anisotropic materials for different directions can be determined not only experimentally, but also through theoretical calculation from the available data. Computer programs designed for this purpose can facilitate the calculation procedure. Through theoretical calculation, the assumed properties of the fabric layer saturated with the matrix can also be determined, as long as the values E_i, μ_i, and G_i for the individual layer components are known. This means E_i, μ_i, and G_i reinforcements for all the necessary directions and values of the matrix, which mostly exhibits isotropic behavior.

V. MODELING IN ABAQUS

The samples were modeled according to the template in the form of the tested samples. Several approaches were offered. The given samples can be modeled as flat shells, to which the thickness of the individual layers will be assigned. Another option is to model a solid 3D body with a specified thickness that corresponds to the theoretically calculated thickness of the sample in question. In load simulations, the second variant is more effective, as it more realistically displays the modeled body. A sample sketch is initially created, to which the function *extrusion* later assigns the required thickness.
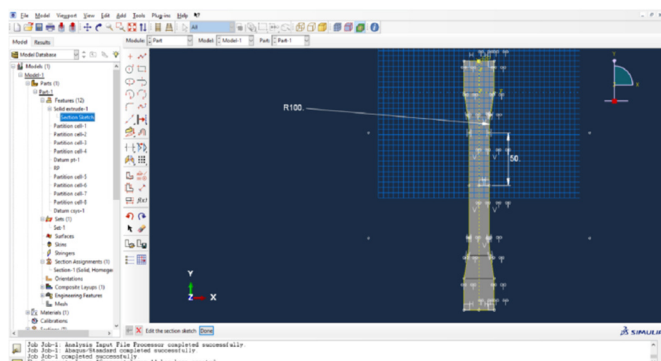

Fig. 8. Creating a sketch of a general sample (the dimensions in the image may not correspond to the final dimensions in the simulation).

Next, the model will be divided into cells, which will allow for a better simulation of a real test. Individual materials are then created. Since in most cases these are anisotropic materials, the modulus of elasticity and Poission's number must be stated separately for each direction as the so-called engineering constants (*E1*, *E2*, *E3*, *Nu12*, *Nu13*, *Nu23*, *G1*, *G2*, *G3*). All the necessary materials that were considered in the samples will be created. Input parameters from producers' datasheets and other available sources are used, whereas in some cases, values obtained by previous calculations are employed. If the acquired input data represented an interval of values, the lowest values were chosen. The tool *Composite Layup* was utilized to stack the individual layers on top of each other, assigning them a material, and determining their relative thickness within the sample and other parameters.
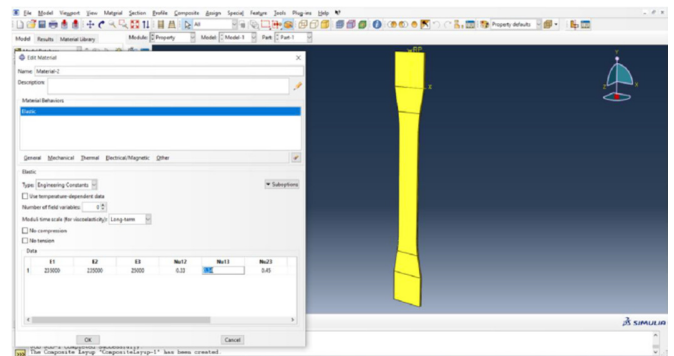

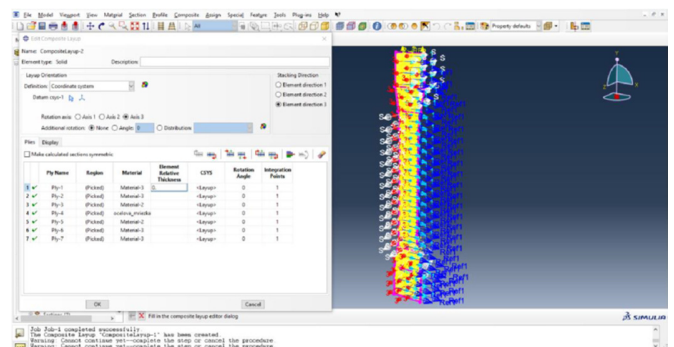Fig. 9. Creating a material with anisotropic properties.

Fig. 10. Creating individual layers in Abaqus.

Further operations followed in the Abaqus interface. Their aim was to make the simulation as close as possible to the conditions to which the sample was exposed during a real test in the laboratory. A single force was then created, placed at the reference point, and was assigned the necessary magnitude and direction. It is necessary to ensure that the reference point is connected to the modeled sample. This will be realized with the assistance of a tool named Coupling. In the Load module. The weaving of the sample was also simulated into the jaws of the tearing device. The key to the finite element method is to create the sample mesh before running the calculations and simulate loading. The student version of Abaqus limits the creation to a maximum of 1000 nodes.
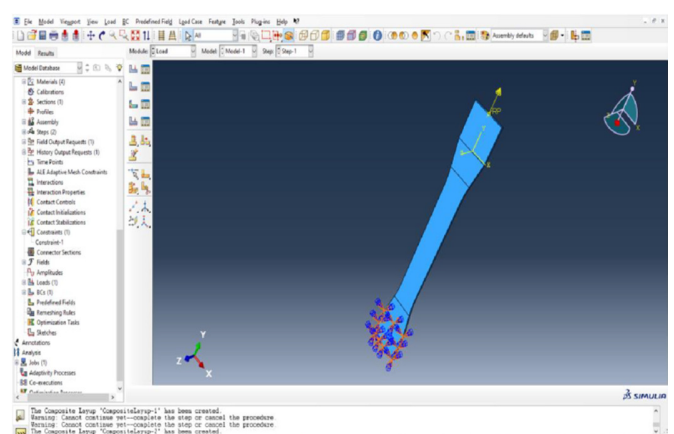

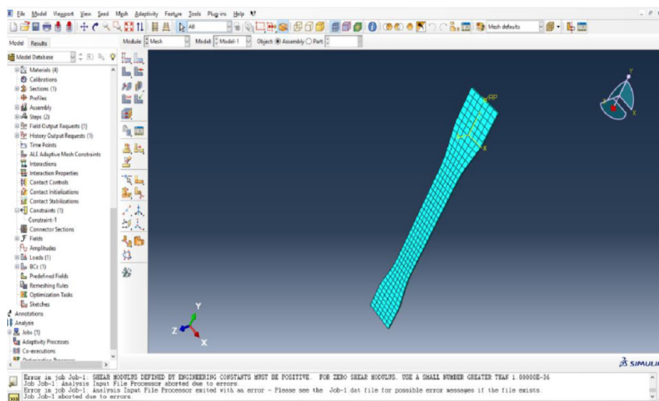Fig. 11. Loading of the sample with the required force and weaving it.

Fig. 12.   Created mesh in the Mesh module in the Abaqus interface.

VI.   TENSILE LOAD SIMULATION AND PROGRESS EVALUATION

A correctly modeled and loaded body will be subjected to a simulated test in the Job module. During the evaluation of the results, several inconsistencies and errors emerged. In Abaqus, it is not a problem to go back to previous incorrectly entered data entries and correct them. The same applies to changes in the sample type, when the element was not necessary to be modeled anew, but changing some previous data in the program or make other minor alterations or corrections was enough. From the simulation in Abaqus, based on calculations using the finite element method, values that describe the mechanical properties of the bodies and other important data can be acquired.
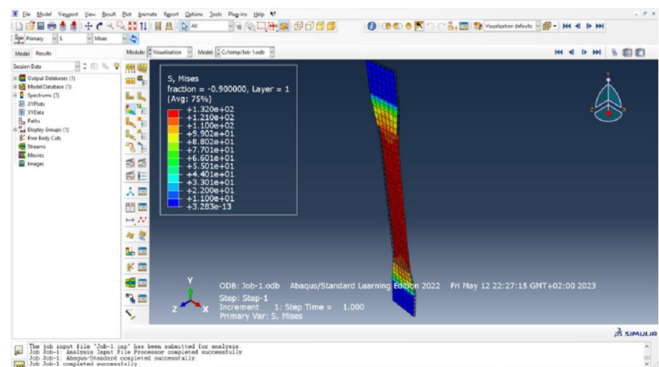

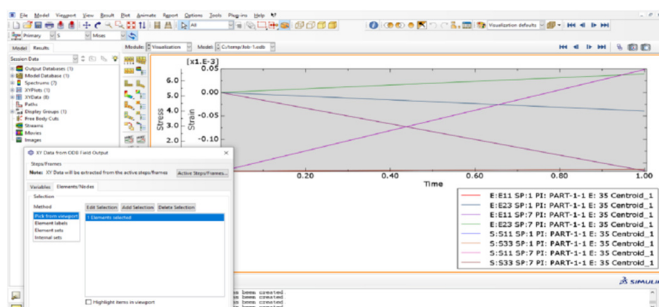Fig. 13.   Visualization of the loaded sample looks in Abaqus.

Fig. 14.   Plotting the required data in Abaqus.

An approach was chosen in which a universal sample was modeled. For each specific case, a middle layer material was assigned to it. The parameters of the other layers did not change and their relative thickness was only adjusted depending on the sample. A gradual increase of the tensile force was performed manually and the values for comparison with real tests were read. The Step module can make this work easier. It allows to set steps to the required amount of force. In the resulting tables, a force of 0.5, 1.0, 1.5, 2.0, 3.0, 4.0, 5.0, and 6.0 kN was selected for each type of sample.

VII.   RESULT COMPARISON

Regarding the tensile tests of the samples in question, during the tests, the tensile force was increased until the sample was torn. The elongation of the sample and the force at which the failure occurs were evaluated. Subsequently, other parameters were calculated (Rm, maximum tension, etc.). For the needs of this paper, the value of sample elongation ΔL will be compared. The elongation caused by a force ranging between 0.5 kN and 6 kN will be investigated. This investigation will be conducted due to the absence or questionable accuracy of the available information that would allow for a reliable simulation of the sample behavior just before failure and in the area of plastic deformation. The effect of the force on the sample is not continuously assessed, but for better clarity 8 values of loading force were selected and listed for the individually tested samples.

A.   Type A Sample Test (Glass Fiber)

In the case of type A samples, whose middle layer was made of glass fiber fabric laid at an angle of 45° highly uniform results were generally achieved. The first two test samples differed only minimally, whereas the third showed a smaller elongation of a maximum of 0.02 mm, depending on the applied force. Compared with the tensile test simulation in the Abaqus program, the results of the real tested samples are very similar in some cases, for example, under a load of 2.0 kN, the third test sample (A-3) exhibits the same elongation value as calculated by the software.

TABLE I.   COMPARISON OF ΔL WITH RESPECT TO F FOR TYPE A SAMPLE

Sample	Elongation ΔL [mm] of sample under force [kN]								Violation at force [N]
	0.5	**1.0**	**1.5**	**2.0**	**3.0**	**4.0**	**5.0**	**6.0**	
A-1	0.11	0.15	0.20	0.25	0.34	0.43	0.53	0.62	7182
A-2	0.12	0.17	0.22	0.26	0.35	0.44	0.53	0.62	7451
A-3	0.10	0.15	0.19	0.24	0.33	0.42	0.52	0.60	8352
A-Simul.	0.09	0.14	0.19	0.24	0.32	0.41	0.50	0.58	…

Accurate data collected from several sources concerning the matrix, the glass, and carbon fibers were used in the production of the type A sample. Thanks to this fact, it was possible to achieve a relatively accurate simulation of the tested sample. Small deviations from the theoretical model also indicate relatively precise work in the production of the sample, despite the limiting conditions.

B. Test Sample Type B (Aramid Honeycomb)

The first of the tested samples of type B displayed from the beginning the lowest elongation values compared to the other two. Nevertheless, at an applied force of 4531 N, it ruptured prematurely (unexpectedly). Due to the specific situation, this case will not be assessed and compared with the other tested samples, nor with the results achieved in the simulation software. The second and third tested samples of type B illustrate, as in the case of A samples, very similar values, approximately up to the magnitude of the applied force of 6 kN. Compared to the theoretical simulated model, the measured elongation values are higher. The difference is 0.05 mm on average and approximately increases linearly with increasing load.

TABLE II.   COMPARISON OF ΔL WITH RESPECT TO F FOR TYPE B SAMPLE

Sample	Elongation ΔL [mm] of sample under force [kN]								Violation at force [N]
	0.5	1.0	1.5	2.0	3.0	4.0	5.0	6.0	
B-1	0.09	0.15	0.20	0.24	0.33	0.43	-	-	4531
B-2	0.12	0.16	0.20	0.25	0.34	0.43	0.53	0.61	6531
B-3	0.11	0.16	0.20	0.25	0.34	0.44	0.53	0.62	7047
B-Simul.	0.07	0.11	0.15	0.19	0.28	0.36	0.45	0.54	…

C. Type C Sample Test (Hybrid Fabric)

Samples marked as type C have a hybrid fabric of different types of fibers in their core. Compared to the carbon and glass fabrics used in the examined samples, this hybrid aramid layer has lower values of the quantities describing the strength and stiffness of the material. At the same time, however, the fabric is thicker (more mass per unit area), thanks to which the sample withstands greater forces. This was confirmed in the real tests, as it was necessary to develop the greatest force for rupture of all cases, but due to the larger cross-sectional area, thinner samples of type A and B were able to withstand higher tension. Very similar results were achieved for all three tested samples. Abaqus calculated lower elongation values than those found in the real tests. The difference was initially 0.04 mm and with increasing force it increased to 0.08 mm. After loading with higher forces, i.e. when approaching the area of plastic deformation, the difference in real and simulated elongation decreases, but due to missing input data, these values were no longer evaluated.

TABLE III.   COMPARISON OF ΔL WITH RESPECT TO F FOR SAMPLE TYPE C

Sample	Elongation ΔL [mm] of sample under force [kN]								Violation at force [N]
	0.5	1.0	1.5	2.0	3.0	4.0	5.0	6.0	
C-1	0.13	0.17	0.21	0.25	0.32	0.40	0.48	0.55	8598
C-2	0.13	0.17	0.20	0.25	0.33	0.40	0.49	0.56	8312
C-3	0.12	0.16	0.20	0.24	0.32	0.40	0.48	0.55	8844
C-Simul.	0.08	0.12	0.15	0.19	0.27	0.34	0.42	0.51	…

Similarly to the aramid honeycomb samples, the C-type samples have tensile elongation values in the simulation software that differ from the values obtained during the real test. The results could be influenced by the production

technology. The materials vendor recommends making composites in a way that requires elevated temperature. However, the preparation of the samples for testing was carried out at room temperature, which could have resulted in worse final characteristics than expected.

D. Type D Sample Test (Metal Grid 2 × 2 mm)

D-type patterns are significantly different from the previous ones in terms of structure. They contain a steel grid in the core, with a grid size of 2 x 2 mm. Samples of type A, B, and C were completely non-metallic, which creates a more striking difference considering the material. The first and third tested samples achieved similar values of elongation under different loads, and were also broken at a similarly high applied force. The second tested (D-2) sample demonstrated a notably higher elongation even from small forces. However, it did not require less force to tear it apart than in the other two. Therefore, an error in the tensile test can be assumed, specifically in the measurement with a strain gauge. For this reason, the simulation results will not be compared with the second tested sample of type D.

TABLE IV.   COMPARISON OF ΔL WITH RESPECT TO F FOR TYPE D SAMPLE

Sample	Elongation ΔL [mm] of sample under force [kN]								Violation at force [N]
	0.5	1.0	1.5	2.0	3.0	4.0	5.0	6.0	
D-1	0.10	0.14	0.19	0.24	0.33	0.41	0.50	0.59	7955
D-2	0.24	0.29	0.33	0.38	0.46	0.55	0.64	0.73	7844
D-3	0.12	0.16	0.25	0.25	0.34	0.43	0.51	0.60	8034
D-Simul.	0.10	0.14	0.18	0.21	0.28	0.35	0.42	0.46	…

At smaller loads (up to 2 kN), the difference in the elongation value obtained by simulation and real tests is minimal and comparable to the differences observed with the previous types of samples. From a loading force of 3 kN, the difference remarkably increases and at a force of 6 kN it is almost 0.2 mm. At higher forces, outside the considered range, the difference grew even more. The reason for the result variation is likely to be incorrect input data, the cause of which is a lack of information about the metal grid used. The modeling of a specific grid in the simulation software was not performed, but values from the available literature were utilized for the same grid size as the one employed in production. Their mechanical properties probably differ due to the steel used or the production technology.

E. Type E Sample Test (10 x 10 mm Metal Grid)

The last type of sample tested is similar to type D, with the difference in the size of the grid employed. In real tensile tests, uniform results were achieved without significant deviations. Equivalently to the previous case of D samples, a significant difference compared to the simulations in the Abaqus software was observed. The differences in elongation increase again with increasing force and do not correspond to realistically achieved results at high loads.

As with the load simulations of type D samples, there were no further information available about the implemented steel grid. An emphasis was placed on the experimentally determined parameters of the mechanical properties of the

metal grid with the same dimensions emerging from the available literature. To achieve more accurate results, it would be necessary to know the exact properties of the grid used in the production of the sample and to model the entire structure in the simulation software.

TABLE V.   COMPARISON OF ΔL WITH RESPECT TO F FOR TYPE E SAMPLE

Sample	Elongation Δl [mm] of sample under force [kN]								Violation at force [N]
	0.5	1.0	1.5	2.0	3.0	4.0	5.0	6.0	
E-1	0.09	0.13	0.17	0.22	0.29	0.38	0.47	0.56	6538
E-2	0.10	0.14	0.18	0.23	0.31	0.38	0.48	0.57	7745
E-3	0.09	0.15	0.18	0.23	0.30	0.38	0.47	0.56	8038
E-simul.	0.07	0.10	0.13	0.17	0.23	0.29	0.35	0.42	…

VIII. DISCUSSION

At low applied forces, the sample elongation values during the real and the simulated tests are very similar. In some cases, the theoretical value even coincided with the measured one. As the force increased, the difference between the simulation and the real test increased. This could have been caused by the deviation of the materials' input parameters from reality. Type D and E samples with a metal grid constituted an exception. For those, the values obtained by simulation crucially differed from the measured ones, mainly due to the incorrect values of the modulus of elasticity or the Poisson's number, which we used due to the lack of information about the implemented grids. Table VI presents a comparison of the elongation differences between the samples. The ΔL reference value of the physical tests of each sample for comparison with the simulation results was determined as the average value calculated from the aforementioned tables of the test results.

TABLE VI.   COMPARISON OF THE ΔL DIFFERENCE BETWEEN REAL TESTS AND SIMULATION

Sample		Elongation Δl [mm] of sample under force [kN]							
		0.5	1.0	1.5	2.0	3.0	4.0	5.0	6.0
A - glass fiber	Real test	0.11	0.15	0.20	0.25	0.34	0.43	0.53	0.61
	Simulation	0.09	0.14	0.19	0.24	0.32	0.41	0.50	0.58
	Difference	**0.02**	**0.01**	**0.01**	**0.01**	**0.02**	**0.03**	**0.03**	**0.03**
B - aramid honeycomb	Real test	0.11	0.16	0.20	0.25	0.34	0.43	0.53	0.61
	Simulation	0.07	0.11	0.15	0.19	0.28	0.36	0.45	0.54
	Difference	**0.04**	**0.05**	**0.05**	**0.06**	**0.06**	**0.07**	**0.08**	**0.07**
C - hybrid aramid-carbon	Real test	0.13	0.17	0.20	0.25	0.32	0.40	0.48	0.55
	Simulation	0.08	0.12	0.15	0.19	0.27	0.34	0.42	0.51
	Difference	**0.05**	**0.05**	**0.05**	**0.06**	**0.05**	**0.06**	**0.06**	**0.04**
D - metal grid 2×2 mm	Real test	0.11	0.15	0.23	0.24	0.34	0.42	0.50	0.59
	Simulation	0.10	0.14	0.18	0.21	0.28	0.35	0.42	0.46
	Difference	**0.01**	**0.01**	**0.05**	**0.03**	**0.06**	**0.07**	**0.08**	**0.13**
E - metal grid 10×10 mm	Real test	0.09	0.14	0.17	0.22	0.29	0.38	0.47	0.56
	Simulation	0.07	0.10	0.13	0.17	0.23	0.29	0.35	0.42
	Difference	**0.02**	**0.04**	**0.04**	**0.05**	**0.06**	**0.09**	**0.12**	**0.14**

The highest differences in the measured values were noticed for samples Type D and E, which were reinforced with a metal grid. Relatively more accurate findings were measured for Type A samples, where the reinforcement was glass fiber. A number of factors could have caused these differences in the measured values. In [29-30], research has been conducted in the field of integrating composite materials with other material types for selected applications in the automotive industry. The authors note that composite materials in automotive body structures showcase high potential, especially in the context of reducing vehicle weight, fuel consumption, and emissions during the vehicle's lifespan. Considering the fact that despite the significant efforts of automotive manufacturers and the implementation of regulations and standards, emissions production during vehicle operation has not significantly decreased over the past 10 years, the utilization of various composite and lightweight materials in automotive body construction is exceptionally pertinent.

When evaluating the results, it is necessary to take into account the fact that the tested samples were neither professionally produced, nor at a certified workplace. Also, the manufacturers of the components for composites usually recommend production technologies with an increased solidification temperature in the final production phase, which

can affect the resulting mechanical properties of the finished product. In this study, the production process took place at room temperature.

The importance of the difference in the behavior of the examined samples during the physical test and in the simulation software should be also highlighted. In literature, the individual parameters of the materials' mechanical properties were provided as an interval, in particular the values of Young's modulus of elasticity in tension. Each time, for the simulation purposes, the interval's lowest value is chosen. If the middle or highest value within the interval was to be estimated, there would be an even greater deviation from the real results. However, it is also necessary to consider the questionable accuracy of the declared mechanical properties of the materials in question. It is not an exception if the strength and stiffness parameters of the materials stated by the manufacturer are deliberately overestimated, due to the existing competition on the market with carbon or aramid fibres. Therefore, to obtain more accurate results, it is better to start from experimental data collected through independent tests of the given materials.

Another factor that could cause a greater difference in the measured and simulated values is the actual cross-sectional

area of the samples. Theoretically calculated thicknesses based on the existing data were used in the simulation program. The real thickness of the tested sample may be a bit larger, which was confirmed by measuring several randomly selected samples, without, though, further investigating this fact. It is also questionable why this difference with the theoretical value occurred. However, it will probably be a consequence of the limited possibilities in the sample production. If measurements were to be taken on a larger cross-sectional area and at the same time the thickness of the individual layers was to be accordingly increased, the differences between the measurement and the simulated results would be slightly augmented.

The main objective of the current study was to compare selected properties of hybrid composite materials and their simulations. These comparisons revealed that the results of the simulations and the real tests yielded different outcomes for various combinations. These outcomes were on the one hand influenced by the accuracy of the technological procedure applied to individual samples and on the other hand by the precise specification of material properties entered into the simulation program for each simulation. The research in this area builds upon previous work, which focused on the physical testing of composite material samples under tension and flexure. Further research in this direction needs to focus on refining sample preparation and accurately identifying the properties of individual materials. Additionally, simulation testing of similar samples under flexural stress is planned.

IX. CONCLUSION

Utilizing simulation software is a fast, relatively cheap, and effective way of evaluating material mechanical properties. It enables testing of several samples in a short time as well as dynamic change of material input parameters, sample dimensions, or other data. Unlike real tests, simulations do not require expensive equipment or special premises. In the same way, potential problems in the preparation of the tested samples or the actual test implementation are eliminated. An indisputable advantage in the case of computer simulations is the absence of safety risks associated with the stress tests. The disadvantage may be the questionable reliability of the results and the need for a large amount of high-quality input data to achieve satisfactory accuracy of the findings. In both cases, the human factor affects the tests' correct execution. That is, there may be errors in the production of test samples and subsequent testing, whereas numerical errors may emerge during data entry or element modeling.

The comparison of the selected properties of hybrid composite materials obtained from the real tests with the results obtained by simulations is crucial for ensuring the accuracy and reliability of the computational models. Through the validation of simulation models, cost and time-efficient analysis, enhanced understanding of material behavior, and optimization of design parameters, researchers can leverage both experimental and computational approaches to advance the development of hybrid composite materials for a wide range of engineering applications. Continued interdisciplinary research efforts are essential to further improve the accuracy and reliability of simulation-based predictions, driving innovation in the field of composite material science and engineering.

In this paper, it was possible to achieve simulation results, which largely coincided with the physical tests in the laboratory. At the same time, however, it is evident that the calculations of the bearing capacity of materials using the finite element method are very sensitive to the accuracy of the input data. At first glance, small and negligible deviations of the boundary conditions and parameters at the input can lead to a significant deviation of the obtained results from reality. This factor can cause inaccuracies, especially in the case of anisotropic materials, such as the subject hybrid composites, since a larger number of input parameters are needed to simulate their behaviour. This gives the opportunity for more deviations to occur. Nevertheless, it is necessary to point out the prudent approach selected when choosing the input parameters. If less discrete values were to be selected from the intervals and the ideal course of physical tests was to be counted, a greater difference would arise between the results. The availability of the necessary input data and their plausibility are also key factors. As it turned out in the practical part of the work, the insufficient quality and quantity of necessary data leads to inaccuracies, which are most visible especially with larger loads.

For common practice in automobile production, or in general in mechanical engineering as well as other engineering fields, it seems to be the most advantageous to combine both approaches in a balanced way. It is necessary to assess when a real test of the mechanical properties of materials is appropriate, and when a simulated test is more suitable, which, however, carries the risk of inaccuracy of the output data. A correct assessment of this issue could lead to significant cost optimization of both the development and production processes.

REFERENCES

[1] N. Ahmad and F. Ahmad, "The Effect of Iron Content on the Thermodynamic Properties of Syndiotactic Polypropylene/Iron Composites," *Engineering, Technology & Applied Science Research*, vol. 13, no. 5, pp. 11785–11788, Oct. 2023, https://doi.org/10.48084/etasr.6241.

[2] L. Tesfaye Jule, K. Ramaswamy, N. Nagaprasad, V. Shanmugam, and V. Vignesh, "Design and analysis of serial drilled hole in composite material," *Materials Today: Proceedings*, vol. 45, pp. 5759–5763, Jan. 2021, https://doi.org/10.1016/j.matpr.2021.02.587.

[3] A. E. Magri, K. El Mabrouk, S. Vaudreuil, and M. E. Touhami, "Mechanical properties of CF-reinforced PLA parts manufactured by fused deposition modeling," *Journal of Thermoplastic Composite Materials*, vol. 34, no. 5, pp. 581–595, May 2021, https://doi.org/10.1177/0892705719847244.

[4] B. Wang, S. Zhong, T.-L. Lee, K. S. Fancey, and J. Mi, "Non-destructive testing and evaluation of composite materials/structures: A state-of-the-art review," *Advances in Mechanical Engineering*, vol. 12, no. 4, Apr.

2020, Art. no. 1687814020913761, https://doi.org/10.1177/1687814020913761.

[5] P. Zhang, Y. Feng, T. Q. Bui, X. Hu, and W. Yao, "Modelling distinct failure mechanisms in composite materials by a combined phase field method," *Composite Structures*, vol. 232, Jan. 2020, Art. no. 111551, https://doi.org/10.1016/j.compstruct.2019.111551.

[6] D. Gay, *Composite Materials: Design and Applications*, 4th edition. Boca Raton, FL, USA: CRC Press, 2022.

[7] P. Kumar and A. Kumar, "Bending Analysis of Steel-Concrete Composite Beams with Porosity," *Engineering, Technology & Applied Science Research*, vol. 13, no. 4, pp. 11230–11234, Aug. 2023, https://doi.org/10.48084/etasr.6050.

[8] P. K. Penumakala, J. Santo, and A. Thomas, "A critical review on the fused deposition modeling of thermoplastic polymer composites," *Composites Part B: Engineering*, vol. 201, Nov. 2020, Art. no. 108336, https://doi.org/10.1016/j.compositesb.2020.108336.

[9] F. Pierron and M. Grédiac, "Towards Material Testing 2.0. A review of test design for identification of constitutive parameters from full-field measurements," *Strain*, vol. 57, no. 1, 2021, Art. no. e12370, https://doi.org/10.1111/str.12370.

[10] S. Yuan, S. Li, J. Zhu, and Y. Tang, "Additive manufacturing of polymeric composites from material processing to structural design," *Composites Part B: Engineering*, vol. 219, Aug. 2021, Art. no. 108903, https://doi.org/10.1016/j.compositesb.2021.108903.

[11] G. D. Goh, Y. L. Yap, H. K. J. Tan, S. L. Sing, G. L. Goh, and W. Y. Yeong, "Process–Structure–Properties in Polymer Additive Manufacturing via Material Extrusion: A Review," *Critical Reviews in Solid State and Materials Sciences*, vol. 45, no. 2, pp. 113–133, Mar. 2020, https://doi.org/10.1080/10408436.2018.1549977.

[12] T. H. Ibrahim, I. A. S. Alshaarbaf, A. A. Allawi, N. K. Oukaili, A. El-Zohairy, and A. I. Said, "Theoretical Analysis of Composite RC Beams with Pultruded GFRP Beams subjected to Impact Loading," *Engineering, Technology & Applied Science Research*, vol. 13, no. 6, pp. 12097–12107, Dec. 2023, https://doi.org/10.48084/etasr.6424.

[13] Y. Ivanova, "Damage Detection in Free–Free Glass Fiber Fabric Composite Beams by measuring Flexural and Longitudinal Vibrations," *Engineering, Technology & Applied Science Research*, vol. 13, no. 3, pp. 10685–10690, Jun. 2023, https://doi.org/10.48084/etasr.5788.

[14] C. Han *et al.*, "Microstructure and mechanical properties of (TiB+TiC)/Ti composites fabricated *in situ* via selective laser melting of Ti and B4C powders," *Additive Manufacturing*, vol. 36, Dec. 2020, Art. no. 101466, https://doi.org/10.1016/j.addma.2020.101466.

[15] N. Naveed, "Investigating the Material Properties and Microstructural Changes of Fused Filament Fabricated PLA and Tough-PLA Parts," *Polymers*, vol. 13, no. 9, Jan. 2021, Art. no. 1487, https://doi.org/10.3390/polym13091487.

[16] V. Mahesh, S. Joladarashi, and S. M. Kulkarni, "A comprehensive review on material selection for polymer matrix composites subjected to impact load," *Defence Technology*, vol. 17, no. 1, pp. 257–277, Feb. 2021, https://doi.org/10.1016/j.dt.2020.04.002.

[17] C. Hu and Q.-H. Qin, "Advances in fused deposition modeling of discontinuous fiber/polymer composites," *Current Opinion in Solid State and Materials Science*, vol. 24, no. 5, Oct. 2020, Art. no. 100867, https://doi.org/10.1016/j.cossms.2020.100867.

[18] O. Falco, R. L. Avila, B. Tijs, and C. S. Lopes, "Modelling and simulation methodology for unidirectional composite laminates in a Virtual Test Lab framework," *Composite Structures*, vol. 190, pp. 137–159, Apr. 2018, https://doi.org/10.1016/j.compstruct.2018.02.016.

[19] Y. Wan and J. Takahashi, "Development of Carbon Fiber-Reinforced Thermoplastics for Mass-Produced Automotive Applications in Japan," *Journal of Composites Science*, vol. 5, no. 3, Mar. 2021, Art. no. 86, https://doi.org/10.3390/jcs5030086.

[20] *The Aluminum Automotive Manual. Applications – Car body – Body structures*. European Aluminium Association, 2013.

[21] Y. Liu, "Application of Carbon fiber-reinforced plastic composite material in automotive bumper," *IOP Conference Series: Earth and Environmental Science*, vol. 692, no. 2, Nov. 2021, Art. no. 022057, https://doi.org/10.1088/1755-1315/692/2/022057.

[22] T. Kyono, "Life Cycle Assessment of Carbon Fiber-Reinforced Plastic," in *High-Performance and Specialty Fibers: Concepts, Technology and Modern Applications of Man-Made Fibers for the Future*," 1st ed., Tokyo, Japan: Springer, 2016, pp. 355–361.

[23] L. Gornet and H. Ijaz, "A high-cyclic elastic fatigue damage model for carbon fibre epoxy matrix laminates with different mode mixtures," *Composites Part B: Engineering*, vol. 42, no. 5, pp. 1173–1180, Jul. 2011, https://doi.org/10.1016/j.compositesb.2011.03.004.

[24] N. Bouhfid *et al.*, "Numerical modeling of hybrid composite materials," in *Modelling of Damage Processes in Biocomposites, Fibre-Reinforced Composites and Hybrid Composites*, M. Jawaid, M. Thariq, and N. Saba, Eds. Sawston, UK: Woodhead, 2019, pp. 57–101.

[25] R. Thandavamoorthy and A. Palanivel, "Testing and Evaluation of Tensile and Impact Strength of Neem/Banyan Fiber-Reinforced Hybrid Composite," *Journal of Testing and Evaluation*, vol. 48, no. 1, pp. 647–655, Jan. 2020, https://doi.org/10.1520/JTE20180640.

[26] R. Beigpour, H. Shokrollahi, and S. M. R. Khalili, "Experimental and numerical analysis of a biodegradable hybrid composite under tensile and three-point bending tests," *Composite Structures*, vol. 273, Oct. 2021, Art. no. 114255, https://doi.org/10.1016/j.compstruct.2021.114255.

[27] T. H. Gonsalves, M. K. Garje Channabasappa, R. Motagondanahalli Rangarasaiah, and S. Joladarashi, "Dynamic characterization of hybrid composite material of rotor-bearing support system," *Mechanics of Advanced Materials and Structures*, vol. 29, no. 16, pp. 2342–2357, Jun. 2022, https://doi.org/10.1080/15376494.2020.1861667.

[28] Y. L. Tee, C. Peng, P. Pille, M. Leary, and P. Tran, "PolyJet 3D Printing of Composite Materials: Experimental and Modelling Approach," *JOM*, vol. 72, no. 3, pp. 1105–1117, Mar. 2020, https://doi.org/10.1007/s11837-020-04014-w.

[29] D. Sabadka and S. Kender, "Unconventional Methods of Joining Composites and Metals in the Context of Weight Reduction of Car Bodies," *Advances in Science and Technology Research Journal*, vol. 17, no. 1, pp. 230–242, 2023, https://doi.org/10.12913/22998624.

[30] E. E. Evin, M. Tomas, A. Mares, D. Sabadka, and S. Kender, "The selection of materials for automotive deformation zones," *Transfer Innovations*, vol. 40, pp. 36–41, 2019.